ELSEVIER

Ceramics International 32 (2006) 283–289

CERAMICS INTERNATIONAL

www.elsevier.com/locate/ceramint

Nonlinear electrical behaviour of the Cr_2O_3, ZnO, CoO and Ta_2O_5-doped SnO_2 varistors

F.M. Filho [a], A.Z. Simões [a,*], A. Ries [a], L. Perazolli [a], E. Longo [b], J.A. Varela [a]

[a] *Instituto de Química, UNESP, C.P. 355, 14800-900 Araraquara, SP, Brazil*
[b] *Laboratório Interdisciplinar de Eletroquímica e Cerâmica, Departamento de Química, UFSCar, C.P. 676, 13565-905 São Carlos, SP, Brazil*

Received 29 October 2004; received in revised form 2 January 2005; accepted 8 March 2005
Available online 13 May 2005

Abstract

The effects of Cr_2O_3 on the properties of (Zn, Co, Ta)-doped SnO_2 varistors were investigated in this study. The samples with different Cr_2O_3 concentrations were sintered at 1400 °C for 2 h. The properties of (Zn, Co, Ta, Cr)-doped SnO_2 varistors were evaluated by XRD, dilatometry, SEM, *I–V* and impedance spectroscopy. DC electrical characterization showed a dramatic increase in the breakdown electrical field and in the nonlinear coefficient with the increase in Cr_2O_3 concentration. The grain size was found to decrease from 13 to 5 μm with increasing the Cr_2O_3 content. The impedance data, represented by means of Nyquist diagrams, show two time constants, one at low frequencies and the other at high frequencies.

Keywords: E. Varistors; Tin dioxide; Chromium

1. Introduction

Varistors are materials whose current–voltage characteristics are nonlinear. They are used both as protecting devices against voltage transients in electronic and industrial equipment and as surge arrestors [1]. Commercial varistors used in protection systems are based on SiC (silicon carbide) or on ZnO (zinc oxide). SiC-based varistors have low nonlinearity coefficients ($\alpha = 5$) where α is the nonlinearity constant defined by the relation of $I = KV^{\alpha}$, where I is current, V is voltage and K is a proportionality constant [2]. The ZnO-based varistors have very high nonlinearity coefficients ($\alpha = 50$) and their major phase consists of ZnO and of small amounts of Bi_2O_3, Sb_2O_3, CoO, MnO_2 and Cr_2O_3 [3,4]. The reaction between the ZnO and the additives at high temperatures leads to the formation of several phases in the grain boundary of ZnO [5,6]. Thus, despite their chemical composition and phases, the type of processing employed, as well as the sintering temperature, heating and cooling rates are fundamental to control and understand electrical properties of this ceramic [7]. In view of this fact, the literature contains extensive reports describing the influence of processing variables on the properties and mechanisms that govern these system properties [8–14]. Other varistor systems based on $SrTiO_3$ [15] TiO_2 [16] and, more recently, WO_3 varistors [17] have been described in the literature, but the nonlinearity of these systems is very low ($2 < \alpha < 12$) compared with that of the multicomponent ZnO varistors. Pianaro et al. [18] were the first to present an SnO_2-based system as the main candidate to substitute multicomponent ZnO varistors.

Tin dioxide (SnO_2) is an n-type semiconductor with rutile type crystalline structure and has low densification rate due to its high surface tension as diffusion coefficient at low temperatures and high SnO_2 partial pressure at high temperatures [19]. Dense SnO_2-based ceramics can be achieved by introducing dopants or by hot isostatic pressure processing [20]. The addition of CoO creates oxygen vacancies and Co'_{Sn} or Co''_{Sn} which can segregate at the grain

* Corresponding author. Tel.: +55 16 3301 6600; fax: +55 16 3322 7932.
E-mail address: alezipo@yahoo.com (A.Z. Simões).

0272-8842/$30.00
doi:10.1016/j.ceramint.2005.03.004

boundaries [21]. Both defects can help the formation of the Schottky barriers at grain boundaries. The function of ZnO is the creation of oxygen vacancies and Zn''_{Sn} defects [22]. The latter are less segregated and contribute to the Schottky barrier formation. However, both additives lead to a highly resistive material. The addition of tantalum oxide creates $Ta^{\bullet}_{Sn}$ defect (donor) that increase the lattice conductivity of SnO_2-based ceramics [21]. Moreover, in small concentrations Ta_2O_5 does not segregate at the grain boundaries resulting in a high grain conductivity. Excess of Ta_2O_5 causes segregation of defects at grain boundaries which decrease both, bulk conductivity and grain size. Bueno et al. reported that the varistors of $(98.95 - x)\%$ $SnO_2 + 1.0\%$ $CoO + 0.05\%$ $Nb_2O_5 + x\%$ Cr_2O_3 sintered at 1300 °C for 1 h would lose its nonlinearity when $x = 0.05$ in molar system, due to the possibility of $CoCr_2O_4$ formation at the grain boundaries [23]. The impedance spectroscopy (IS) technique has also been used to study polycrystalline tin oxide specimens. The IS technique allows for the separation of the three main contributions to the electrical conductivity of a polycrystalline solid: bulk, internal surfaces like grain boundaries and electrodes [24]. This is accomplished by varying the frequency of the AC input signal over a wide range in order to cover the different responses that charges carriers have inside grains, at grain boundaries and at the specimen electrode-interface. In our work, the Cr_2O_3-doped SnO_2 ceramics were prepared using ZnO and CoO as densification mediators and Ta_2O_5 to increase the electric conductivity. The effect of chromium oxide on the structural, morphological and electrical properties of the $SnO_2{\cdot}ZnO{\cdot}CoO{\cdot}Ta_2O_5$ (SZCT) varistors was investigated. As a result, an optimum composition was obtained.

2. Experimental procedure

The powder was prepared using the mixed oxide method in alcoholic medium. All the oxides used were analytical grade: SnO_2 (Cesbras-Fine), ZnO (Synth) CoO (Riedel), Ta_2O_5 (Aldrich), Cr_2O_3 (Vetec). The molar composition of the investigated systems was $(98.95 - x)\%$ $SnO_2 + 0.50\%$ $CoO + 0.50\%$ $ZnO + 0.05\%$ $Ta_2O_5 + x\%$ Cr_2O_3, with x equal to 0.025, 0.050 and 0.075 mol%. The amounts of CoO and ZnO were always kept constant, because this additives were used to facilitate densification during sintering. The powder was pressed into pellets by uniaxial pressing followed by isostatic pressing at 210 MPa. The pellets were sintered at 1400 °C for 2 h in oxygen atmosphere and slowly cooled to room temperature (5 °C/min). The X-ray data were collected with a Rigaku-2000 diffractometer under the following experimental conditions: copper anode, 50 kV, 150 mA, Cu Kα radiation monocromatized by a graphite crystal. The tetragonal structure (rutile structure) of the SnO_2 starting material was confirmed by X-ray diffraction. Mean grain size was determined by analyzing the SEM micrographies (Topcom Sm-300). To perform the electrical measurements, silver contacts were deposited on the samples surfaces. Current–tension measurements were taken using High Voltage Measure Unit (Keithley Model 237). The breakdown electric field (E_b) was obtained at a current density from 1 mA cm^{-2}.

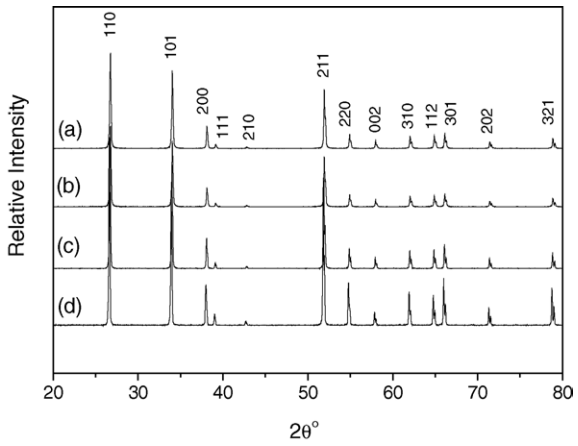

Fig. 1. X-ray diffraction data of the varistor system doped with different chromium concentrations: (a) without Cr; (b) 0.025 mol%; (c) 0.050 mol%; (d) 0.075 mol%.

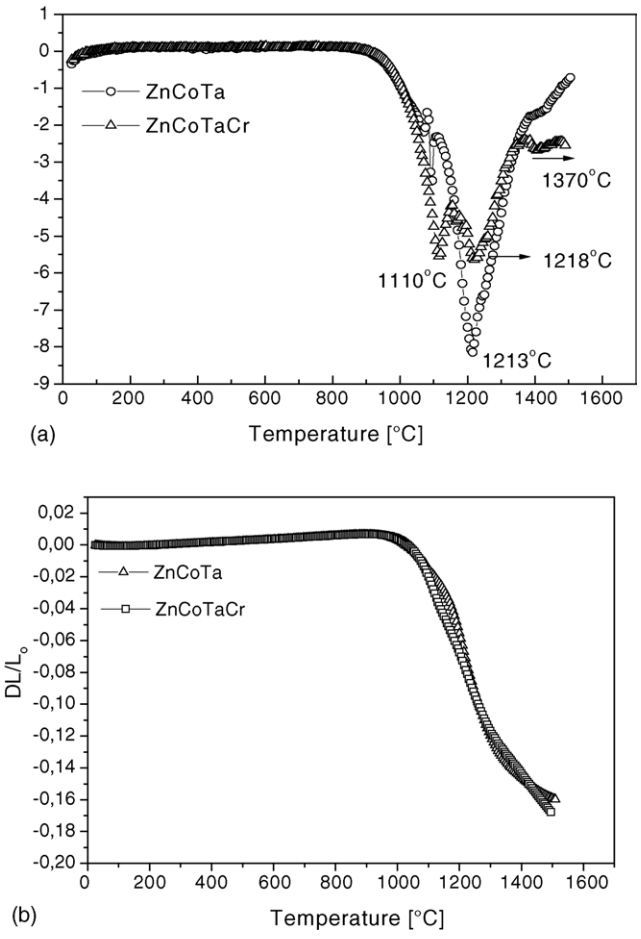

Fig. 2. (a) Linear shrinkage rate and (b) linear retraction for different dopant concentrations as a function of temperature.

The impedance measurements were made with a frequency response analyser using frequency ranging from 100 Hz up to 4 MHz, with an amplitude voltage of 1 V. The pellets were put in a sample holder attached to a furnace. Measurements of real (Z') and the imaginary (Z'') were made at temperatures ranging from 225 to 350 °C. The impedance data were analysed with the EQUIVCRT program [25].

3. Results and discussion

Fig. 1 shows the X-ray diffraction analysis of a SnO_2-based varistor system with a molar concentration of 0.50% CoO + 0.50% ZnO + 0.05% Ta_2O_5 and several amounts of Cr_2O_3. Besides the SnO_2 rutile phase, no secondary phase was observed. A sintering study combined with XRD results indicated that sintering at 1400 °C for 2 h are the optimal conditions to obtain crystalline, dense Cr_2O_3·Ta_2O_5·CoO·ZnO-doped SnO_2 varistors containing only the expected rutile phase. The amount of additives is too small and other possible phase might not be detected because of the detection limit of the XRD equipment. All dopants introduced in the SnO_2 matrix lead to a stable solid solution according to the Eqs. (1)–(5).

$$ZnO \longrightarrow SnO2ZnSn'' + V0\bullet\bullet + O0x \quad (1)$$

$$CoO \xrightarrow{SnO_2} Co''_{Sn} + V_0^{\bullet\bullet} + O_0^x \quad (2)$$

$$Co_2O_3 \xrightarrow{SnO_2} 2Co''_{Sn} + 2V_0^{\bullet\bullet} + 2O_0^x \quad (3)$$

$$2Ta_2O_5 \xrightarrow{SnO_2} 4Ta^{\bullet}_{Sn} + V''''_{Sn} + 10O_0^x \quad (4)$$

$$Cr_2O_3 \xrightarrow{SnO_2} 2Cr'_{Sn} + V''''_0 + 3O_0^x \quad (5)$$

The linear shrinkage rate ($d(\Delta l/l_0)/dT$) and linear variation $\Delta l/l_0$ as a function of temperature for the samples SnO_2 + 0.5%CoO + 0.5%ZnO + 0.05% Ta_2O_5 and SnO_2 + 0.5%CoO + 0.5%ZnO + 0.05% Ta_2O_5 + 0.05% Cr_2O_3 are presented in Fig. 2. The presence of two peaks close to

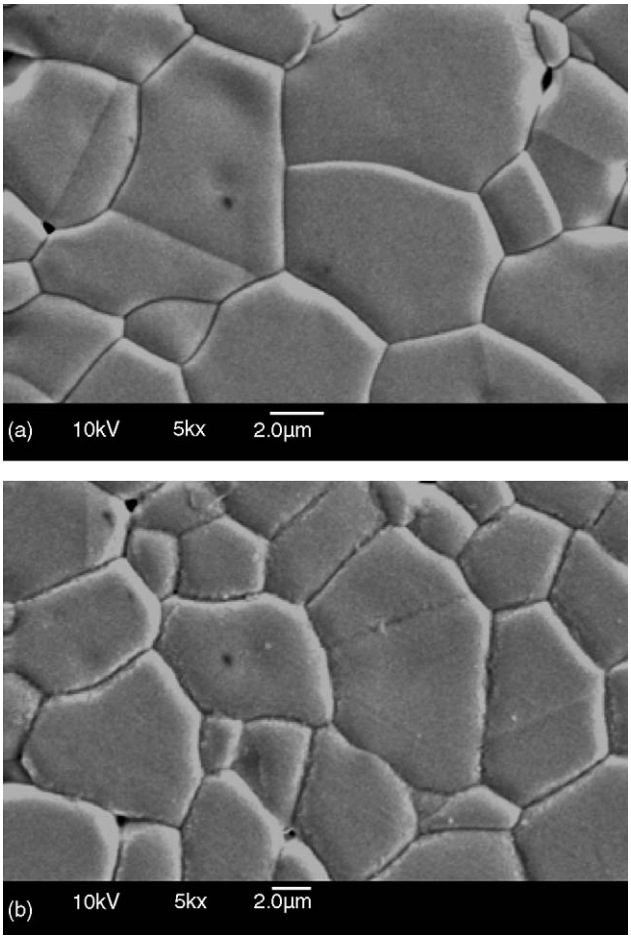

Fig. 3. SEM micrographs for the SZCT system doped with different chromium concentrations: (a) without Cr; (b) 0.05 mol%.

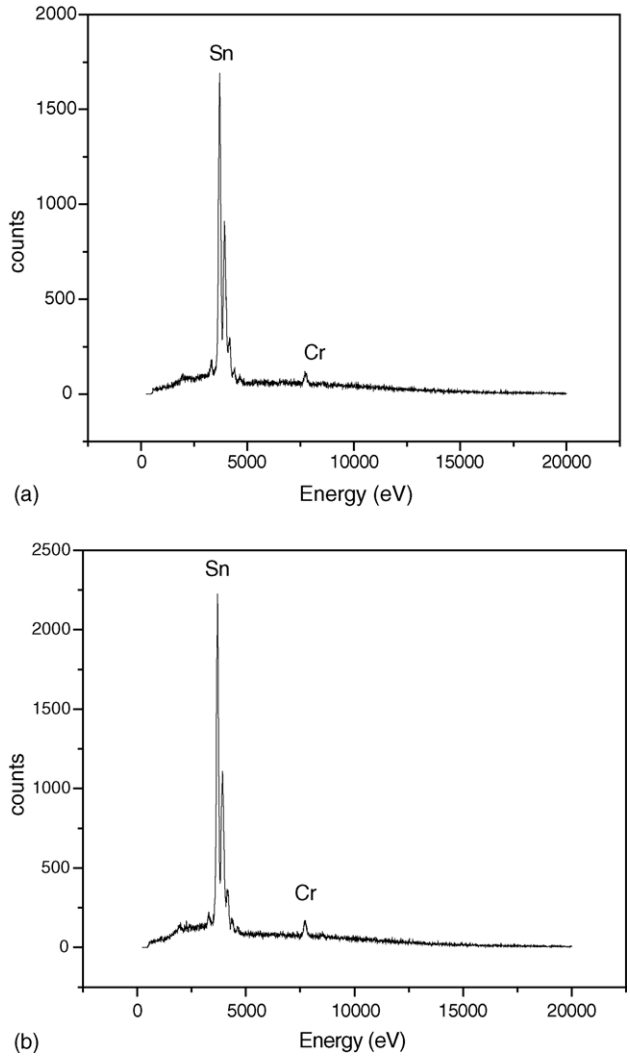

Fig. 4. EDS analyses for the sample 98.9% SnO_2 + 0.5 mol% CoO 0.5 mol% ZnO + 0.05 mol% Ta_2O_5 + 0.05 mol%Cr_2O_3: (a) grain; (b) grain boundary.

Table 1
Influence of the Cr_2O_3 on the relative densities, grain sizes, nonlinear coefficients (α) and breakdown fields (E_b) for the SZCT system

SnO_2	CoO	ZnO	Ta_2O_5	Cr_2O_3	ρ_r (%)	(α)	E_b (V/cm)	V_b (V/barrier)	Average grain size (μm)
98.95	0.5	0.5	0.05	–	98.5	11.5	1100	1.49	13.5 ± 2.2
98.93	0.5	0.5	0.05	0.025	98.8	15.0	2800	2.52	9.0 ± 2.1
98.90	0.5	0.5	0.05	0.050	98.5	20.4	3050	2.41	7.9 ± 2.4
98.88	0.5	0.5	0.05	0.075	98.3	21.5	5000	2.50	5.0 ± 2.2

1110 °C and 1220 °C for the sample doped with Cr_2O_3 indicates that during the first stages of the sintering process occurs a structural change leading to the formation of intra and inter-agglomerates. This modification is due to the different particle size obtained from the raw powders. Another peak close to 1370 °C could arise from defects on the grain boundaries or from a possible SnO_2 evaporation. This suggests a possible $CoCr_2O_4$ segregation at the grain boundaries. The increase in chromium concentration has strong influence on the sintering process of the system. For the sample doped with 0.05% in Cr_2O_3, there is a segregation at the grain boundaries shifting the maximum shrinkage temperature to 1218 °C which results to a decrease in grain size. The same behaviour was observed for the samples doped with other Cr_2O_3 concentrations.

Fig. 3 shows the SEM micrograph of two systems considered in this study. Although no secondary phases were observed in SEM micrographs, $CoSnO_3$ and $CoCr_2O_4$ could be precipitated at the grain boundaries leading to a decrease in the grain size with the increase in chromium concentration. However, electron dispersive spectroscopy revealed that there is no difference in dopant concentration between grain and grain boundary (Fig. 4). A high amount of trapped pores in the grains may be the result of the slow grain growth rate during sintering. The densities of sintered samples were obtained by the Arquimedes method and are related to the

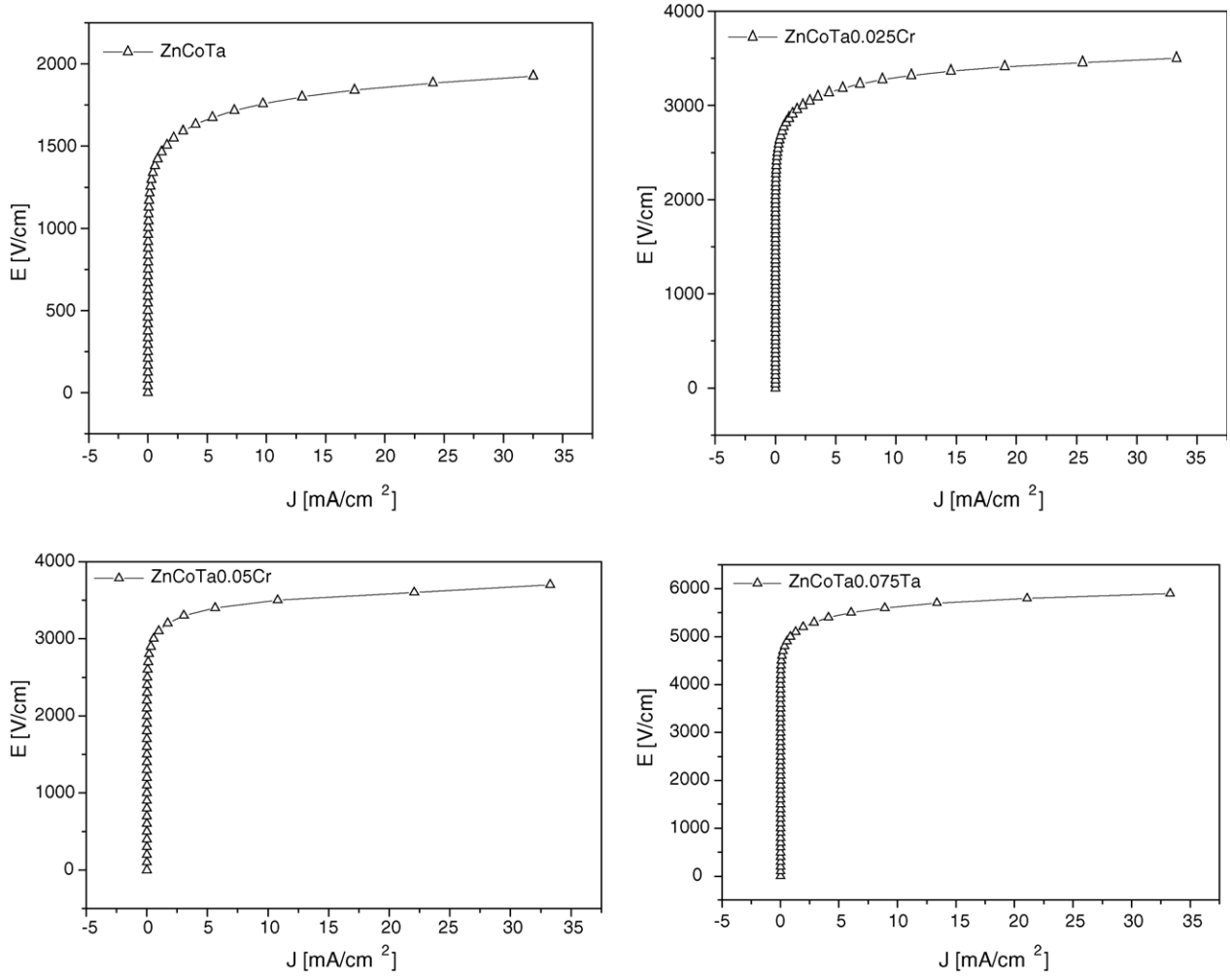

Fig. 5. Applied electric field as a function of current density for the SZCT system doped with different chromium concentrations: (a) without Cr; (b) 0.025 mol%; (c) 0.050 mol%; (d) 0.075 mol%.

theoretical density of SnO_2 ($\rho_{theoretical}$ = 6.95 g/cm^3). The final densities after sintering are higher than 98%, as shown in Table 1. They were only slightly affected by variations of the Cr_2O_3 content, although the average grain size decreased significantly with an increase in Cr_2O_3 concentration. The high densification of tin dioxide ceramics was attributed to the zinc and cobalt effect in the SnO_2 lattice, which leads to the formation of oxygen vacancies according to the Eqs. (1), (2) and (3). If one considers that diffusion of oxygen vacancies is the rate controlling step, the substitution of Sn^{4+} by Zn^{2+}, Co^{2+} or Co^{3+} increases the sintering rate of SnO_2 ceramics.

The applied electric field as a function of current density for the different systems is given in Fig. 5. The nonlinear coefficient α was obtained by $\alpha = \log(I_2/I_1)/(V_2/V_1)$ where V_1 and I_1 as well as V_2 and I_2 are corresponding values of voltage and current for two points that can be chosen arbitrarily [26]. The α values were obtained from the curves $E \times J$ for current densities between 1 and 10 mA cm^{-2}. The highest nonlinear coefficient (α = 21.5) was obtained when molar concentrations of 0.075 mol% Cr_2O_3 were added to SnO_2, presenting an electric breakdown field of 5000 V/cm. It was observed that the addition of Cr_2O_3 in concentrations varying from 0.025 to 0.075 mol% leads to a substantial modification in the electrical behavior of the SnO_2·Z-*ZnO*\cdot*CoO*\cdot-·CoO·Ta_2O_5 ceramics. The electric behaviour of the system without Cr_2O_3, although nonlinear, is highly resistive. The samples containing 0.075 mol% Cr_2O_3 are more resistive (electrical breakdown close to 5000 V/cm) and possess a nonlinear coefficient equal to 21.5. Comparing the results presented in Table 1 and Fig. 5, it can be concluded that the increase in Cr_2O_3 concentration decreases the grain size increasing the nonlinear coefficient and the breakdown electric field. Similar results were found in Bueno article where they described the DC electrical behavior of the SCN and SCNCr systems as a function of different molar Cr_2O_3 concentrations. SCN presents a varistor behavior with α equal to 58 and a breakdown electric field (E_b) of 1870 V/cm. When 0.05% Cr_2O_3 was added to the system, the α value decreased to 41 and the breakdown field increased to 3990 V/cm [23].

Fig. 6a shows the Nyquist diagrams of SZCTCr with 0.05% Cr_2O_3 at four different temperatures. The semicircles observed in Fig. 6 were obtained by convolution of two time constants in the system. So, the electrical response can be fitted by an equivalent electrical circuit composed by two series circuits of a resistance and capacitor in parallel, as shown in Fig. 6b. Two hypotheses may be considered to explain these two time constants: The first hypothesis suggests that one time constant is related to the grain boundary barrier and the second is associated with the grain

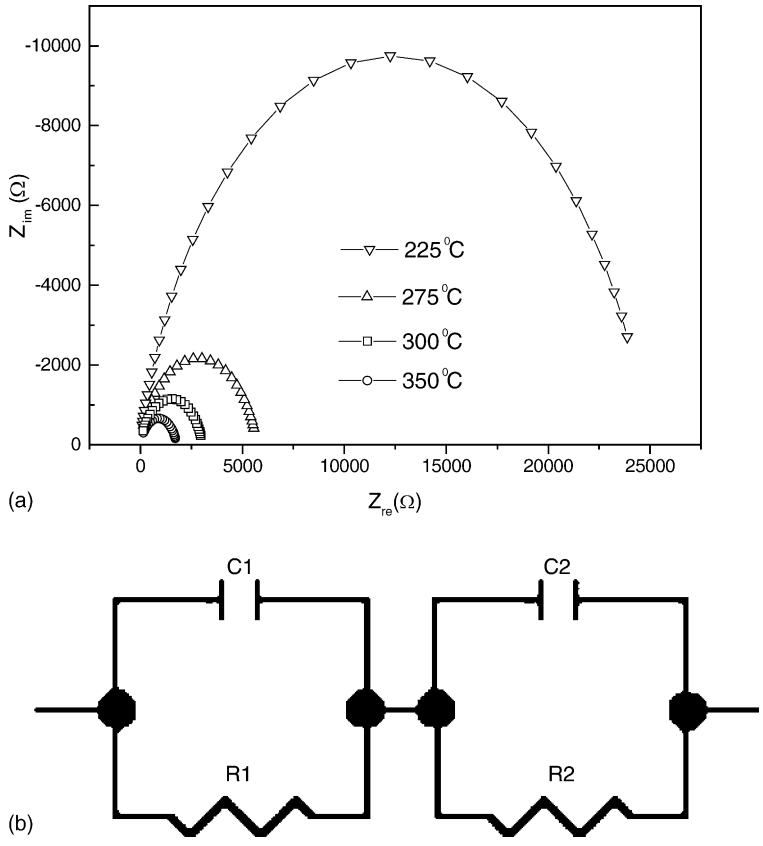

Fig. 6. (a) Nyquist diagrams for SCTCr with 0.05% of Cr_2O_3 at different temperatures and (b) equivalent circuit used to fit the impedance data with two time constants.

barrier. The weakness of this model is that the grain resistivity thus calculated is at least four orders of magnitude higher than the literature values for grain resistivity of SnO_2 [27]. The second hypothesis supposes the existence of different defects and/or adsorbed species at the grain boundary region, not necessarily at the same grain boundary. The two time constants are due to these kinds of defects. The second hypothesis is more probable, since the possibility of existence of different adsorbed species and defects on SnO_2 was described in the literature [28]. Kim et al. [29] observed that for the SCNCr compounds at temperatures higher than 200 °C it is possible that these species predominate at the grain boundary structure and its formation can be represented by the following reactions:

$$Cr2O3 \longrightarrow SnO22CrSn\prime + V0\bullet\bullet + 3O0x \quad (6)$$

$$Cr'_{Sn} + O_2 \xrightarrow{SnO_2} Cr'_{Sn}O_{2(ads)} \quad (7)$$

$$Cr'_{Sn}O_{2(ads)} \xrightarrow{SnO_2} Cr^{x}_{Sn}O'_{2(ads)} \quad (8)$$

$$Cr^{x}_{Sn}O'_{2(ads)} + Cr'_{Sn} \xrightarrow{SnO_2} (Cr^{x}_{Sn})_2O''_{2(ads)} \quad (9)$$

$$(CrSnx)2O2(ads)\prime\prime \longrightarrow SnO22(CrSnxO2(ads)\prime) \quad (10)$$

$$(Cr^{x}_{Sn})_2O'_{2(ads)} + Cr'_{Sn} \xrightarrow{SnO_2} (Cr^{x}_{Sn})_2O''_{2(structural)} \quad (11)$$

The chromium addition promotes the reduction of O'_2 and O' and the reduction of O' to O''. The influence of Cr'_{Sn} is to increase the O' to O'' adsorption at the grain boundary interface and to promote a decrease in the conductivity by donating electrons to O_2 adsorbed at the grain boundary. The absorption of the O'_2 and O' species must take place at the grain boundaries, otherwise no electrical nonlinearity could be observed. From these results one may say that the species that are truly responsible for the barrier formation are O' to O''. The Cr'_{Sn} generates the sites to promote the adsorption of electrophilic species. These defects, O' to O'', are not equally present at the same grain boundary. One of them is probably predominant at a grain. This behavior leads to a random distribution of both defects, and to different charge transport paths in the sample.

Table 1 shows the influence of Cr_2O_3 concentration on the average grain size. The mean grain size was obtained by the intercept method. There are significant differences in average grain size with the increase in Cr_2O_3 concentration. It was observed that the increase of Cr_2O_3 amount introduced in the matrix results probably in a segregation at the grain boundaries which might decrease the grain boundary mobility leading to a decrease in the grain size. These results are in agreement with those of Pianaro et al. [30] who observed the segregation of Cr_2O_3 in the grain boundaries for the system SnO_2*CoO*Ta_2O_5. The grains are regularly distributed with an average grain size from 5.0 to 13.45 μm (Table 1). The mean values of α, E_b and the numbers of effective voltage barriers (V_b) are displayed in Table 1. The effective voltage barriers were determined using the expression: $V_b = E_b n$, where n is the number of grains in a line of length L and G is the mean grain size. The V_b can be estimated as $V_b = E_b G/L$ [31]. Higher breakdown electric field E_b due to the reduced grain size and higher barrier voltage per grain V_b were obtained for Cr_2O_3, ZnO, CoO and Ta_2O_5-doped SnO_2 varistors. There was a decrease in the number of effective barriers of the system doped with 0.050 mol% in Cr_2O_3.

4. Conclusions

The physical characterization showed that all the systems presented high densifications. The experimental results indicated that α and E_b of the SZCT varistor system depend on the Cr_2O_3 concentration. A high nonlinear coefficient of 21.5 for the SnO_2 varistor doped with 0.075 mol% Cr_2O_3 was obtained. The increase in the breakdown electrical field with increasing Cr_2O_3 doping is mainly attributed to the decrease of the grain size. The impedance results show the existence of two time constants in the varistor system investigated. The results suggest different kinds of defects in the grain boundary region.

Acknowledgments

The authors gratefully acknowledge the financial support of the Brazilian agencies FAPESP, CNPq, and CAPES and of the German Academic Exchange Service (DAAD).

References

[1] L.N. Levinson, H.R. Philipp, Zinc oxide varistor — a review, Ceram. Bull. 65 (1986) 639–646.
[2] T. Masuyama, Effect of cobalt(II) oxide and manganese(IV) oxide on sintering of tin(IV) oxide, Jpn. J. Appl. Phys. 7 (1968) 1294–1298.
[3] M. Matsuoka, Nonohmic properties of zinc oxide ceramics, Jpn. J. Appl. Phys. 10 (1971) 736–745.
[4] E.R. Leite, M.A.L. Nobre, E. Longo, J.A. Varela, Microstructural development of ZnO varistor during reactive liquid phase sintering, J. Mater. Sci. 31 (1996) 5391–5398.
[5] M. Inada, Crystal phases of non-ohmic zinc oxide ceramics, Jpn. J. Appl. Phys. 17 (1978) 1–10.
[6] M. Inada, Microstructure of nonohmic zinc oxide ceramics, Jpn. J. Appl. Phys. 17 (1978) 673–677.
[7] M. Inada, Formation mechanism of nonohmic zinc oxide ceramics, Jpn. J. Appl. Phys. 19 (1980) 409–419.
[8] L.N. Levinson, H.R. Philipp, Physics of metal-oxide varistors, J. Appl. Phys. 46 (1975) 1332–1341.
[9] P.L. Hower, T.K. Gupta, Barrier model for ZnO varistors, J. Appl. Phys. 50 (1979) 4847–4855.
[10] W.G. Morris, Physical properties of electrical barrier in varistors, Vac. Sci. Technol. 13 (1976) 926–931.
[11] K. Eda, Mechanism of nonohmic zinc oxide ceramics, J. Appl. Phys. 49 (1978) 2964–2972.
[12] K. Eda, A. Tga, M. Matsuoka, Degradation mechanism of nonohmic zinc oxide ceramics, J. Appl. Phys. 51 (1980) 2678–2684.

[13] P.R. Emtage, Statistics and grain-size in zinc oxide varistors, J. Appl. Phys. 50 (1979) 6833–6837.
[14] J. Wong, Barrier voltage measurement in metal-oxide varistors, J. Appl. Phys. 47 (1976) 4971–4974.
[15] N. Yamaoka, M. Masuyama, M. Fukui, $SrTiO_3$-based boundary-layer capacitor having varistor characteristics, Am. Ceram. Soc. Bull. 62 (1983) 698–702.
[16] J.F. Yan, W.W. Rhodes, Preparation and properties of TiO_2 varistors, Appl. Phys. Lett. 40 (1982) 536–537.
[17] V. Makarov, M. Trontelj, Novel varistor material based on tungsten-oxide, J. Mater. Lett. 13 (1994) 937–939.
[18] S.A. Pianaro, P.R. Bueno, E. Longo, J.A. Varela, A new SnO_2-based varistor system, Mater. Sci. Lett. 14 (1995) 692–694.
[19] J.G. Fagan, V.R.W. Amarakoon, Reliability and reproducibility of ceramic sensors: part III, humanity sensors, Am. Ceram. Soc. Bull. 72 (1993) 119–130.
[20] S.J. Park, K. Hirota, H. Yamamura, Enhanced sintering of tin dioxide with additives under isothermal condition, Ceram. Int. 10 (1984) 115–116.
[21] J.A. Cerri, E.R. Leite, D. Gouvea, E. Longo, Effect of cobalt(II) oxide and manganese(IV) oxide on sintering of tin(IV) oxide, J. Am. Ceram. Soc. 79 (1996) 799–804.
[22] A.C. Antunes, S.R.M. Antunes, S.A. Pianaro, M.R. Rocha, E. Longo, J.A. Varela, Nonlinear electrical behavior of the $SnO_2{\cdot}CoO{\cdot}Ta_2O_5$ system, Mater. Sci. Lett. 17 (1988) 577–579.
[23] P.R. Bueno, S.A. Pianaro, E.C. Pereira, E. Longo, J.A. Varela, Investigation of the electrical properties of SnO_2 varistor system using impedance spectroscopy, J. Appl. Phys. 84 (1998) 3700–3705.
[24] B.A. Boukamp, A Nonlinear least square fit procedure for analysis of immitance data of electrochemical systems, Solid State Ionics 20 (1) (1986) 31–44.
[25] S.P. Jiang, J.G. Love, S.P.S. Bbadwal, Electrical properties of oxide materials, Key Eng. Mater. 125 (1997) 81–132.
[26] T.K. Gupta, Application of zinc-oxide varistors, J. Am. Ceram. Soc. 73 (1990) 1817–1840.
[27] Z.M. Jarzebski, J.P. Marton, Physical-properties of SnO_2 materials. 1. Preparation and defect structure, J. Electrochem. Soc. 123 (7) (1976) C199–C205.
[28] T. Arai, The study of the optical properties of conducting tin oxide films and their interpretation in terms of a tentative band scheme, J. Phys. Soc. Jpn. 15 (5) (1960) 916–927.
[29] M.C. Kim, K.H. Song, S.J. Ppark, Isothermal capacitance transient spectroscopy study on trap levels in polycrystalline SnO_2 ceramics, J. Mater. Res. 8 (6) (1993) 1368–1372.
[30] S.A. Pianaro, G.F. Menegotto, A.J. Zara, S.R.M. Antunes, A.C. Antunes, Varistor behavior of the system $SnO_2{\cdot}CoO{\cdot}Ta_2O_5{\cdot}Cr_2O_3$, J. Mater. Sci.-Mater. El. 13 (5) (2002) 253–256.
[31] E.R. Leite, A.M. Nascimento, P.R. Bueno, E. Longo, J.A. Varela, Effect of Cr_2O_3 in the varistor behaviour of TiO_2, J. Mater. Sci. Lett. 15 (1996) 2048–2050.